Heliyon 10 (2024) e37913

Contents lists available at ScienceDirect

Heliyon

journal homepage: www.cell.com/heliyon

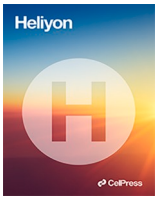

Research article

An evaluation of static ToF-SIMS analysis of environmental organics

Xiao Sui [a], Xiao-Ying Yu [b,*]

[a] College of Geography and Environment, Shandong Normal University, Jinan, 250358, China
[b] Materials Science and Technology Division, Oak Ridge National Laboratory, Oak Ridge, TN, 37830-6136, United States

ARTICLE INFO

Keywords:
ToF-SIMS
Spectral repeatability
Organics
Emulsion
Solvent
Aqueous organic aerosol

ABSTRACT

Time-of-flight secondary ion mass spectrometry (ToF-SIMS) has been extensively used in surface analysis due to its high mass resolution, sensitivity, and mass spectral imaging capabilities. Static ToF-SIMS has mainly been used for solid material analysis; however, its application in environmental organics is limited. During SIMS spectral analysis, relative mass accuracy and measurement repeatability are key factors for obtaining reliable speciation and acquiring chemical insights of the specimens. Herein, we provide an evaluation of four environmentally relevant organic systems, including glyoxal, pyruvic acid, oil-in-water emulsion, and carbon dioxide (CO_2) capture solvent (i.e., N-2-ethoxyethyl-3-morpholinopropan-1-amine, EMMPA), to show the spectral measurement repeatability when using static ToF-SIMS. First, sample preparation is essential in acquiring accurate and reproducible results in ToF-SIMS analysis. The mass spectral results show that characteristic peaks observed can be distinguished with reasonable confidence by comparing the observed mass to charge ratios (m/z) to theoretical ones. The statistical analysis of peak areas indicates that the peak area and/or peak height measurement ratios are satisfactory among replicates. Compared with previous studies, the bismuth cluster primary ion beam, namely Bi_3^+, has less fragmentation than Bi^+. Therefore, Bi_3^+ is deemed more suitable for organic analysis using static SIMS. Our results show that ToF-SIMS offers a viable approach to study environmental organics including but not limited to aqueous aerosols, wastewater emulsions, and CO_2 capture solvents. It is expected that future studies will expand organic speciation with high fidelity due to the continued advancement of SIMS as a sensitive analysis technique.

Abbreviation

EMMPA	N-2-ethoxyethyl-3-morpholinopropan-1-amine
NPL	National Physical Laboratory
PCA	principal component analysis
PDMS	polydimethyl siloxane
RDS%	relative standard deviations percentage
S.D	standard deviation
SEM	scanning electron microscope
SNR	signal to noise ratio
SOAs	secondary organic aerosols

(*continued on next page*)

* Corresponding author.
E-mail address: yuxiaoying@ornl.gov (X.-Y. Yu).

https://doi.org/10.1016/j.heliyon.2024.e37913
Received 26 March 2024; Received in revised form 10 September 2024; Accepted 12 September 2024
Available online 13 September 2024

(*continued*)

ToF-SIMS	time-of-flight secondary ion mass spectrometry
VOCs	volatile organic compounds
VAMAS	versailles project on advanced materials and standards

1. Introduction

Environmental organics have profound effects on the Earth's ecology, human habitat, and public health. Here environmental organics refer to the organics that are observed in the environment and they are closely studied in environmental science and engineering research due to their impact on the greenhouse gas emissions and global climate warming. For example, multiphase oxidation of volatile organic compounds (VOCs) is an important pathway to form secondary organic aerosols (SOAs), which can cause haze formation and affect the global climate's radiative budget and human health [1,2]. The application of large-scale, efficient, and cost-effective carbon dioxide ($CO_{2)}$ capture in existing fossil fuel plants is necessary for the sustainable green chemistry [3–5]. However, large portions of environmental organics are difficult to analyze due to the nature of the molecular complexity and their presence in trace amounts. Particularly, it is the surface composition of these organics that triggers a series of heterogeneous chemical reactions [6–8]. Thus, to further understand the behavior between surface properties and environmental functions, it is essential to characterize the environmental organics surface in detail.

Among surface analysis techniques, time-of-flight secondary ion mass spectrometry (ToF-SIMS) has seen rapid growth in characterization of various environmental samples due to the features of high mass resolution and sensitivity. Additionally, multimodal measurements of SIMS offer chemical mapping of elements, molecules, and isotopes via interactions of the primary ion beam, including static SIMS and in situ liquid SIMS [4,9–16]. Using static SIMS, liquid samples are usually transformed into a solid surface for analysis, similar to what is developed by X-ray photoelectron spectroscopy (XPS) [17]. The initial development of the static SIMS technique can be traced back to the 1970s [18]. The first Versailles Project on Advanced Materials and Standards (VAMAS) interlaboratory study on static SIMS was coordinated by the National Physical Laboratory (NPL). Their results indicated that static SIMS instruments could have good repeatability, better than 18 % [19]. Primary ion beams, such as C_{60}, Ga^+ and Cs^+, are often used in polymeric and organic analysis in early days of SIMS [20,21]. With the advent of ToF-SIMS systems since the mid-1980s, Ga^+ and Ar^+ became popular. Most recently, giant cluster ion beams (i.e., water or carbon oxide) have shown promising results in biological analysis [22,23]. However, their applications in environmental organics are sparse. Most modern ToF-SIMS instruments are equipped with liquid metal ion beams (i.e., Bi_n^+). The single metal ions (e.g., Bi^+) may have significant surface damage and further affect measurement repeatability [24]. Afterwards, several new primary ion beams have emerged for the static SIMS analysis. The popular ion beams include Bi_3^+, C_{60}^+, Ar_n^+ and $(H_2O)_n^+$ that were developed by commercial corporations, such as the IONTOF GmbH, PHI, and Ionoptika [26]. These primary ion beams, such as Bi_3^+, can increase sputter yields and reduce beam damage effectively compared to single metal ions [24]. Static ToF-SIMS has mainly been applied to solid materials like semiconductors, polymers, or metals [20, 27–29]. Much effort has been devoted to biological research such as mammalian cells, microbial biofilms, and plants [30–35]. In contrast, dynamic SIMS is a preferred choice in studying material chemical distributions in three dimensions.

Recently, the effect of environmental organics has caused increased attention as a notable topic concerning interfacial processes. The application space includes, but is not limited to atmospheric aerosol interfacial formation, environmental pollutants, and greenhouse gas emission and reduction [36–39]. An important aspect of SIMS measurements is relative mass accuracy and peak area/height measurement ratios, which establishes the foundation for further analysis, such as principal component analysis (PCA), two-dimensional (2D), or 3D image analysis [40,41]. Good measurement repeatability on one sample with multiple measurements can boost confidence in peak identification and elucidate the key components observed at the material surface and interface [25]. We primarily focus on this type of repeatability comparisons in this study. Therefore, evaluation of spectral repeatability is important to assure the relative mass accuracy as well as subsequent spectral or image analysis. However, a summary on the spectral repeatability of organics of importance in the environment has not been reported to the best of our knowledge despite surging applications of SIMS in organics in recent years [37,38]. Additional future studies regarding interlaboratory comparisons of the same sample or comparisons of multiple samples of the same kind would be of interest to the development of SIMS applications.

To evaluate the spectral repeatability of environmental organics using static ToF-SIMS, we present four representative environmental organic samples including glyoxal, pyruvic acid, bilgewater emulsion and a CO_2 capture solvent (N-2-ethoxyethyl-3-morpholinopropan-1-amine, 2-EMMPA) in this study [36–38,42]. Glyoxal and pyruvic acid are two well studied model systems that are known to form aqueous SOAs that could have significant implications in radiative forcing [37,43]. Oil-in-water emulsions are pollutants in seawater and their interfacial physical, chemical evolutions are challenging to study using bulk techniques [36,44]. CO_2 abatement has become a hot topic in recent years. Understanding CO_2 capture and conversion mechanism using green solvents using SIMS is an attractive approach for building net zero emission and economy [45].

The main objectives of our study are to assess spectral repeatability of environmental organics using static ToF-SIMS. Firstly, sample preparation steps are described to give examples for maximizing the analysis outcome. Second, relative mass accuracy, defined as the relative difference between the observed mass and the theoretical mass (expressed in ppm) using representative pseudo-molecular peaks and fragments are calculated to show measurement reliability [46,47]. Finally, statistical analysis of peak area and peak height is conducted to determine peak area/height measurement ratios. We also illustrate the feasibility of the static ToF-SIMS approach to analyze dry samples of various environmental organics of significance to organic pollutants in the Earth's

atmosphere and ocean water.

2. Materials and methods

2.1. Sample preparation

2.1.1. Silicon substrate preparation

Before sample preparation using photolysis, silicon (Si) wafers were cleaned by using acetone and isopropanol mixed solution (volume ratio 1 to 1) and deionized DI water consecutively. Then the cleaned Si wafer was treated in a UV Ozone plasma cleaner (Ossila, L2002A3-US) to reduce surface contamination from organic compounds [48]. The same process was used to prepare the Si substrate for all organic samples in this work.

2.1.2. Glyoxal aqueous solution

Glyoxal (US 40 % wt.) and hydrogen peroxide (H_2O_2, 30 % wt., certified American Chemical Society, ACS solution in DI water, grade: electrophoresis) were purchased from Thermo Fisher Scientific (9389 Waples St., San Diego, CA 92121). The glyoxal and H_2O_2 solutions were diluted and mixed into a mixture 5 mM and 20 mM, respectively, using DI water with 18.2 MΩ resistivity. DI water was dispensed from a Barnstead™ Nanopure™ system (Thermo Fisher Scientific). The liquid mixture was used to simulate the evaporation and oxidation process of aqSOA formation from glyoxal droplets in the atmosphere [49,50].

Five microliters (μL) of the solution mixture was deposited onto the clean Si wafer surface and then dried using nitrogen (N_2) of ~99 % purity in a chemical fume hood. Liquid samples were deposited three times to form a thin layer of film of several nm on the substrate. A mercury argon (Hg-Ar) UV lamp (ORIEL instruments, lamp model 6035, power supply model 6060, 1791 Deere Avenue, Irvine, CA 92606) was used for photochemical illumination [51]. The distance between the bulb and Si wafer was set at 10 cm to simulate atmospheric illumination based on previous studies as shown in Fig. 1a [40]. Once the desired UV illumination time was reached, dry samples were analyzed by ToF-SIMS immediately. A series of UV exposure times, including 15 min, 30 min, 1 h, 2 h, 4 h, 6 h, and 8 h, were performed to simulate the photochemical reactions of glyoxal and hydroxyl radicals in the atmosphere. In this study, the 6 h illumination sample was used for mass spectral repeatability analysis.

2.1.3. Pyruvic acid aqueous solution

Pyruvic acid (98 %) was purchased from Sigma-Aldrich (St. Louis, MO, USA). It was diluted to a 0.1 M solution using DI water and used for simulating UV photolysis induced aqSOA formation. The photolysis treatment and sample drying followed the same conditions and procedures as shown in glyoxal sample preparation in Fig. 1c. To study the SOA evolution from photochemical reactions of

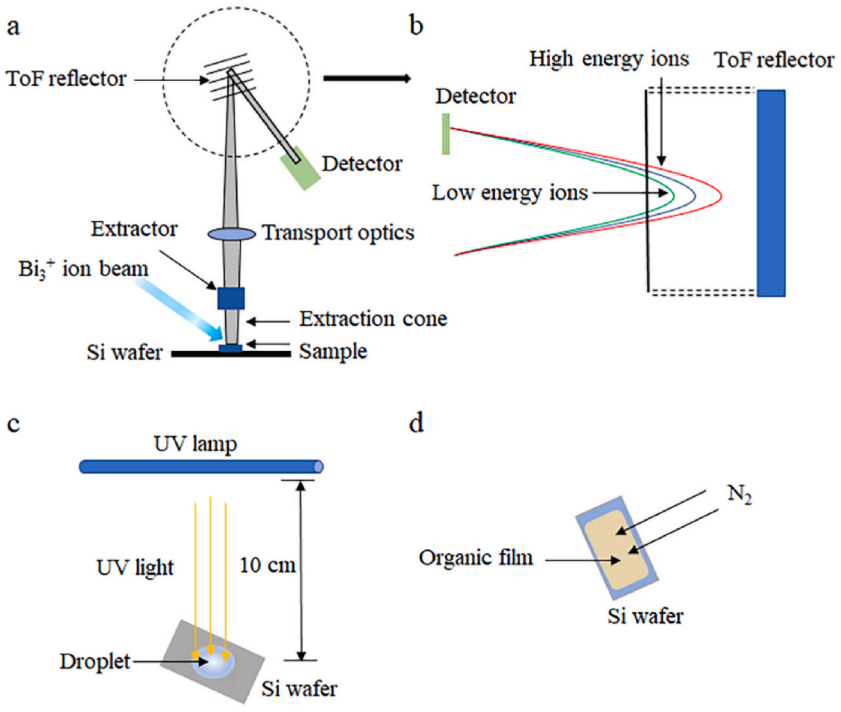

Fig. 1. Schematic showing a) ToF-SIMS cartoon for static analysis of dry samples, b) ToF analyzer with a reflector, c) preparation of aqueous droplet containing glyoxal or pyruvic acid (PA), and d) preparation of thin film of emulsion and EEMPA solvent.

pyruvic acid and hydroxyl radicals, a series of UV exposure times such as 0.5 h, 1 h, 1.5 h, and 2 h were conducted. The 1.5 h UV irradiated pyruvic acid aqueous sample was used for the spectral repeatability analysis.

2.1.4. Synthetic oil-in-water bilgewater emulsion

The emulsions used in this study were synthesized using a 10 mL oil mixture (consisted by 50 % diesel fuel marine, MIL-PRF-16884 N, 25 % 2190 TEP steam lube oil, MIL-PRF-17331K and 25 % 9250 diesel lube oil, MIL-PRF-9000L) and 1 mL detergent mixture (consisted by type 1 general purpose detergent, MIL-D-16791G (1), 25 % commercial detergent Tide Ultra (liquid), and 25 % degreasing solvent, MIL-PRF-680C, Type III). The synthetic bilgewater emulsion was prepared by a homogenizer (Omni Tissue Master, Model 125, 10 mm generator probe) for 2 min at 35,000 rpm and 10 min at 40 kHz sonication followed by the recommended procedure [52]. The oil-in-water emulsion droplets formed immediately, and the droplet size distributions were determined using a high resolution optical microscope (Nikon Eclipse TE2000-U).

The freshly prepared emulsion droplets were used to simulate oil-in-water bilgewater emulsions released from shipboard in the sea. Ten microlieter (μL) of the mixture emulsion was deposited onto a clean Si wafer. The droplet was smeared using a blade to spread the material evenly across the substrate. The fresh emulsion was dried by blowing house N_2 over the surface under room temperature and pressure (Fig. 1d).

2.1.5. CO_2 capture solvent 2-EMMPA

The 2-EMMPA solvent for CO_2 capture was synthesized following the procedure reported in previous studies [53,54]. Five μL of the solvent was deposited onto the Si wafer directly [55]. The solvent was dried using house N_2 as depicted in Fig. 1d.

2.2. Static ToF-SIMS analysis

For the four environmental organics mentioned above, two parallel samples were prepared for each type of organic system, namely one for analysis and the other as the backup. Measurement repeatability can be affected by sample charging, topography, and the matrix effect [46]. The matrix effect is defined as an alteration of the analyte response due to interfering and often unidentified component(s) in the sample matrix. However, the matrix effect will not influence results of chemically similar samples if sample preparation and ToF-SIMS analysis are done properly [56,57]. Dried bilgewater emulsions, environmental VOCs samples, and 2-EMMPA solvent were checked using an optical microscope to assure film uniformity. The optical microscope within the SIMS instrument was also used to confirm the sample evenness prior to SIMS analysis. The acquired two-dimensional (2D) SIMS images gave indication that the observed key peaks were well distributed across the surface [37,40]. As to emulsion and EMMPA, the homogeneity of key compounds was reasonable as shown in the 2D image in previous studies [3,36]. Selected 2D images were illustrated in Fig. S1. The samples were analyzed immediately after preparation to avoid possible surface interference and contamination. All measurements were conducted in a ToF-SIMS V instrument (IONTOF GmbH, Münster, Germany). During analysis, the pressure in the main chamber was maintained at $\sim 10^{-8}$ mbar, and it took about half an hour for the vacuum to reach to the desirable condition in the load lock chamber. The primary beam Bi_3^+ was set at 10 kHz pulsing units, 25 kV ion energy. The "high current bunched mode" (with high mass resolution) was used with a spatial resolution of 2–3 μm. The resolution of Si is about 5000 in both positive and negative mode because the environmental organic compounds covered the substrate. Their fragments and matrix complexity may influence the detection and resolution of Si. In contrast, the mass resolution on Si could be higher than 10,000 when a pure Si wafer is analyzed and used to calibrate instrument. The scanned area was 500 × 500 μm^2. The ion dose was kept smaller than 1×10^{12} ion/cm^2. For example, the dose was 2.5×10^{11} ion/cm^2 for analysis of bilgewater emulsions. Data was acquired after 60 scans. During measurements, an electron flood gun with a filament current of 2.20 pA was used for surface charging compensation. Many replicate measurements were conducted per sample during SIMS analysis. Normally, at least four to five data points were collected if the repeatability was not influenced by surface topography and/or other instrument factors [58] based on visual inspection of data. Data acquisitions of each type of organic sample were performed in the same day. The schematic diagram of SIMS analysis setup was illustrated in Fig. 1a and b.

2.3. ToF-SIMS data analysis

The IONTOF Surface Lab software version 6.0 was used to analyze the mass spectral data. Before performing mass calibration, two common peaks CH_3^+ and C_2H^- were used to check mass resolution (observed mass/difference between the observed mass and the theoretical mass, m/Δm) to evaluate the ability of the ToF-SIMS to distinguish masses with close m/z ratios. This value was larger than 5000 in all samples, indicating that the adjacent peaks could be distinguished effectively using the high current bunched mode. The minimally degraded ions (in the four environmental organic samples that have known organic peaks) were used as the primary criterion during peak calibration [46,47]. For example, for pyruvic acid, glyoxal, and bilgewater emulsions, peaks such as m/z^+ 15.02 CH_3^+, m/z^+ 27.02$C_2H_3^+$, m/z^+ 45.03$C_2H_5O^+$, m/z^+ 55.05C_4H_7, and m/z^+ 85.03$C_4H_5O_2^+$ in the positive mode and m/z^- 13.01 CH^-, m/z^- 14.02 CH_2^-, m/z^- 43.02$C_2H_3O^-$, m/z^- 157.01$C_6H_5O_5^-$, and m/z^- 175.02$C_6H_7O_6^-$ in the negative mode were used. As to the 2-EEMPA solvent, peaks such as m/z^+ 18.03 NH_4^+, m/z^+ 42.00 CNO^+, m/z^+ 55.05$C_4H_7^+$, and m/z^+ 85.03$C_4H_5O_2^+$ in the positive mode and m/z^- 26.00 CN^-, m/z^- 43.00 CNO^-, m/z^- 157.01$C_6H_5O_5^-$, and m/z^- 175.02$C_6H_7O_6^-$ in the negative mode, respectively, were used in calibration. After mass calibration, SIMS spectral data were exported, plotted, and integrated using OriginPro® (OriginLab 2018).

As discussed in the following section, three data points were used to evaluate measurement repeatability after excluding outliers based on the analysis of mean, variance, and covariance [59,60]. The observed m/z_{obs} was defined as the center of mass of the related peaks. By calculation, the standard deviation of the center of mass among the three duplicate dataset was at the ppm level. Thus, the

slight variations among the three parallel samples do not affect mass accuracy. The relative mass accuracy statistical analysis of peak area and peak height were performed to determine measurement repeatability on one sample with multiple measurements.

3. Results and discussions

3.1. SIMS spectral analysis in the negative ion mode

It should be noted that more replicates could increase the estimate of average and standard deviation (S.D.) values based on replication statistics [61]. However, as a highly sensitive surface analytical instrument, the ToF-SIMS spectra repeatability can still be affected by subtle differences of sample charging, topography, the matrix effect, and variation in the SIMS signals due to the inherent challenge of exactly reproducing all conditions for SIMS measurement. This would produce one or two outlier spectra compared with other spectra among all detected points based on our experiences.

Replicates do not always contribute equally and independently to the measured variability and can impact the total variability in the analyte system. Although increasing the number of measurements could improve data reliability and decrease the uncertainty in obtaining the mean, the benefits may decline as the repetition increases [62]. There are not thorough repeatability studies reported on environmental samples using SIMS, other repeatability studies based on mass spectrometry of proteomics and other materials suggested that three to four replicates can offer high repeatability and reproducibility, even for complex mixtures [62–64]. Considering the high costs per assay and possible evaporation of organics under vacuum, more than several replications are not a routine practice in static SIMS spectral collection. Therefore, generally we use three replicate measurements from all data points to reduce data after excluding the outlier data points. This also helps reduce the small, random instrument and sample misalignments that may influence the data quality.

The outlier exclusion process for environmental samples in this work normally includes the following considerations: (1) the spectrum with low signal to noise ratio (SNR) or deviant interference (the SNR is significantly low; or interference peaks are evident compared to other spectra of the same specimen from spectral overlay); and (2) the deviations of peak area/height from the mean value are more than 20 %. This process is helpful in peak identification and follow-up analysis. The characteristic peaks selected for the measurement repeatability evaluation of each sample in the negative ion mode were summarized in Table 1. We use the following criteria to select peaks including: 1) peaks that are pseudo-molecular peaks of the major molecules of each analyte system; 2) those peaks that are identified as important reactants, products, or fragments based on previous reports or our own observations [3,36–38], and 3) peaks that have distinctly higher intensities than adjacent peaks. Besides, we avoid interference peaks from polydimethyl siloxane (PDMS) and Si related peaks in peak comparison. The former is common surface contaminant, and the latter reflects signals from the substrate.

Table 1
Identification of key peaks of representative organics in the negative ion mode.

System	m/z^-_{obs} [a]	m/z^-_{the} [b]	Dev. (ppm) [c]	Formula	Peak assignment
Pyruvic acid [d]	85.030	85.028	17.641	$C_4H_5O_2^-$	biacetyl
	113.023	113.023	1.770	$C_5H_5O_3^-$	3-hydroxy-5-methylfuran-2(5H)-one
	146.991	146.992	8.164	$C_4H_3O_6^-$	1-hydroxy-2-oxoethyl hydrogen carbonate
	175.040	175.039	2.857	$C_{10}H_7O_3^-$	oligomers
	198.986	198.987	7.036	$C_7H_3O_7^-$	oligomers
Glyoxal [e]	57.028	57.029	17.535	$C_2HO_2^-$	glyoxal
	97.013	97.013	7.216	$CH_5O_5^-$	$2H_2O...HCO_3$
	158.057	158.057	3.796	$C_7H_{10}O_4^-$	oligomers
	177.058	177.055	16.379	$C_{10}H_9O_3^-$	oligomers
Bilgewater emulsion [f]	101.058	101.060	17.811	$C_5H_9O_2^-$	fatty acid
	104.980	104.982	14.288	$C_4H_9O_3^-$	dicarbonic acid
	149.022	149.023	12.079	$C_8H_5O_3^-$	benzoylformic acid
	255.230	255.232	7.836	$C_{16}H_{31}O_2^-$	n-hexadecanoic acid
	265.152	265.157	18.857	$C_{12}H_{26}O_4P^-$	tributyl phosphate
EMMPA [g]	73.015	73.016	10.135	$C_2H_3NO_2^-$	fragment of 2-EMMPA
	110.054	110.056	18.173	$CH_8N_3O_3^-$	fragment of 2-EMMPA
	163.058	163.059	4.906	$C_4H_9N_3O_4^-$	fragment of 2-EMMPA
	169.059	169.058	5.324	$C_4H_{11}NO_6^-$	fragment of 2-EMMPA

Footnote.

[a] m/z^-_{obs}: *observed* mass to charge ratio.

[b] m/z^-_{the}: theoretical mass to charge ratio.

[c] Dev. (ppm) = Abs ($10^6 \times (m/z^-_{obs} - m/z^-_{the})/m/z^-_{the}$).

[d] $CH_3COCOOH$, molecular weight (MW) 88.06, 0.1 M solution, 1.5 h UV exposed [37].

[e] Mixture of 5 mM CHOCHO (MW 58.04) and 20 mM H_2O_2 (MW 34.01) solution, respectively, after 6 h UV exposure [43].

[f] synthetic oil-*in*-water emulsion, a 10 mL oil mixture consisted of 50 % diesel fuel marine, MIL-PRF-16884 N, 25 % 2190 TEP steam lube oil, MIL-PRF-17331K and 25 % 9250 diesel lube oil, MIL-PRF-9000L and 1 mL detergent mixture including type 1 general purpose detergent, MIL-D-16791G (1), 25 % commercial detergent Tide Ultra (liquid), and 25 % degreasing solvent, MIL-PRF-680C, Type III [44].

[g] $(CH_2)_4ON(CH_2)_3NH(CH_2)_2OCH_2CH_3$, MW 216.32 [36].

First, five key reactant and product peaks were selected consisting of biacetyl (m/z^- 85.03, $C_4H_5O_2^-$), 3-hydroxy-5-methylfuran- 2 (5H)-one (m/z^- 113.02, $C_5H_5O_3^-$), 1-hydroxy-2-oxoethyl hydrogen carbonate (m/z^- 146.99, $C_4H_3O_6^-$), zymonic acid(m/z^- 157.01, $C_6H_5O_5^-$), and oligomers (m/z^- 175.02, $C_6H_7O_6^-$ and m/z^- 198.99, $C_7H_3O_7^-$), which were related to pyruvic acid photolysis for the four organic systems. These peaks were used in spectral repeatability analysis. Fig. 2 gives an example. Spots 1, 2, and 3 indicates three consecutive measurements at three separate locations. Spectra showing the mass range that includes all observed peaks are illustrated in Figs. S8–S9. The relative mass accuracy was calculated to assure peak identification. Table 1 gives the summary of the selected peaks. The calculated relative mass accuracy is smaller than 20 ppm, suggesting that peak identification is dependable. In spectral comparisons, all selected peaks and other high intensity peaks could be observed with similar counts in three replicate measurements as illustrated in Fig. 2, S8 – S9, respectively.

It is not straightforward to do direct quantitative data analysis of ToF-SIMS spectral data due to the fact that the ion yields were influenced by matrix effects [56,58,65]. Thus, ToF-SIMS is generally regarded as a semi-quantitative technique. Nevertheless, it is essential to compare signal intensity among replicate measurements. This is because under the same operating conditions, spectral repeatability can reflect sample uniformity and measurement repeatability, thereby reflecting the adequacy of sample preparation and instrument response to a specimen. Another reason is that relative intensity is an important reference for peak identification. If the characteristic peaks with high intensity of each replicate plots are different, it will be difficult to distinguish the real products compared to the original reactants and molecular fragments in the acquired spectra. Therefore, reducing the peak intensity standard deviation among parallel samples could enhance the relative mass accuracy.

The summary of peak area and peak height of representative peaks is listed in Table 2. Additionally, the peak area and peak height ratios among key products and fragments are reproducible because sample surfaces are flat. Thus, good measurement precisions were obtained for peak identification of these complex organic mixtures when compared with high purity reference chemical spectra. Besides, peak area/height ratios of key products or fragments tend to be reproducible as long as the topographic difference is not significant, that is, sample surface is flat. Such parameters can provide valuable information when the analyst tries to identify organics in mixtures or more complex matrices, especially for samples that are prepared using step-by-step additions of compounds. It should be noted that surface topography and instrument efficiency (e.g., micro channel plate conditions) will influence the total ion yield. To further evaluate repeatability of one sample with multiple measurements, the ratios of peak areas and peak heights of four types of environmental samples are listed in Table 3. The ratios were normalized using the counts of the specific peak divided by total counts of all selected key products and fragments. The ratio was taken from each spectrum; and the variance and mean values were determined based on all measurements. The relative standard deviations percentage (RSD%) of most peak areas and peak heights were smaller than 5 % among samples. As to peak area ratios, the RSDs% are smaller than 2 %. Typically, if the RSD% is 5 % in peak areas, the method would be considered suitable for quantitative analysis [20]. Therefore, our results of diverse organic samples indicate that static ToF-SIMS spectral signal intensity has excellent repeatability. As to peak heights, the RSD% is around 5 % – 10 %, larger than peak area deviation. Additional results in the positive ion mode are summarized in Tables S1–S3. Using peak area for peak identification would be more dependable in measurement evaluation because the intensity for a particular ion is spread over the mass scale owing to imperfect energy compensation and topography effects. Therefore, intensity should be summed. The peak height is consequently a much smaller value with lower signal to noise and poorer repeatability. Thus, we focus on the peak area standard deviation in the subsequent discussion.

The UV treated glyoxal and hydrogen peroxide sample was used to represent the oxidized aqueous droplet surface inductive to

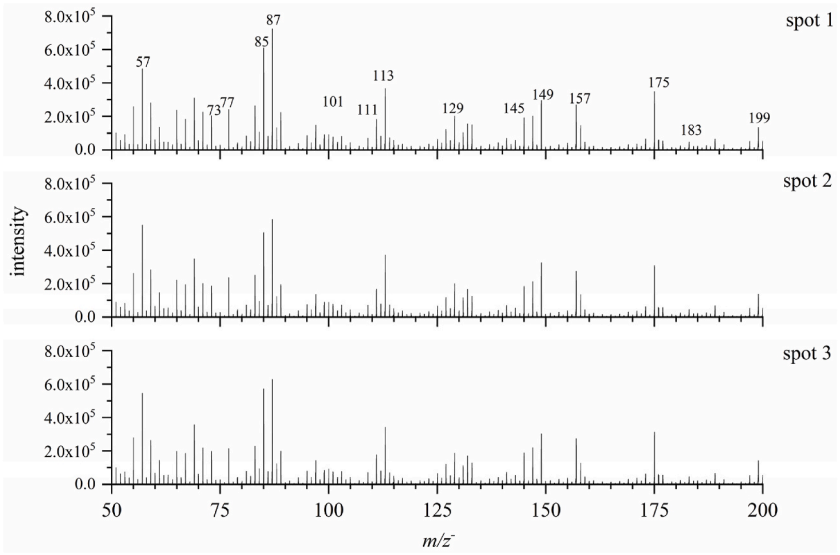

Fig. 2. SIMS spectral comparison of pyruvic acid showing representative peaks in the negative mode (m/z^- 50–200). Spots 1, 2, and 3 indicate consecutive measurements at three separate locations.

Table 2
Summary of peak area and peak height of representative organic peaks in the negative ion mode.

System	m/z^-_{obs}[a]	Peak Area[b]	Area S.D.[c]	Area RSD%[c]	Peak height[d]	Peak height S.D.[e]	Peak height RSD%[e]
Pyruvic acid[f]	85.030	6.43E+03	2.76E+01	0.43 %	5.62E+05	5.30E+04	9.43 %
	113.023	9.64E+03	2.89E+01	0.30 %	3.60E+05	1.54E+04	4.28 %
	146.991	6.28E+03	7.43E+01	1.18 %	2.11E+05	8.73E+03	4.14 %
	175.040	9.84E+03	1.46E+02	1.48 %	3.23E+05	2.11E+04	6.53 %
	198.986	9.04E+03	2.08E+02	2.30 %	1.38E+05	4.01E+03	2.91 %
Glyoxal + H_2O_2[g]	57.028	4.22E+02	1.90E+01	4.50 %	3.55E+04	2.72E+03	7.65 %
	97.007	4.18E+03	1.94E+02	4.65 %	2.68E+05	2.23E+04	8.33 %
	158.057	2.54E+03	7.73E+01	3.05 %	1.07E+05	7.73E+03	7.19 %
	177.058	4.50E+03	1.32E+02	2.93 %	1.08E+05	5.98E+03	5.55 %
Glyoxal[h]	57.027	4.23E+03	1.61E+02	3.80 %	4.29E+05	4.30E+04	10.02 %
	97.008	1.28E+03	5.15E+01	4.01 %	8.64E+04	7.62E+03	8.82 %
	158.049	< S/N	–	–	< S/N	–	–
	177.060	< S/N	–	–	< S/N	–	–
Bilgewater emulsion[i]	101.058	6.78E+02	4.71E+01	6.95 %	1.26E+04	1.48E+04	12.99 %
	104.980	1.36E+03	3.89E+01	2.86 %	1.55E+04	1.12E+04	3.89 %
	149.022	4.07E+03	1.50E+02	3.69 %	4.20E+04	1.59E+03	3.79 %
	255.230	1.95E+03	7.59E+01	3.89 %	2.40E+04	2.48E+04	7.50 %
	265.152	1.36E+03	8.66E+01	4.17 %	1.43E+04	1.40E+04	14.43 %
EMMPA[j]	73.042	2.75E+03	2.59E+02	9.40 %	6.19E+04	8.23E+03	13.29 %
	110.054	2.62E+03	1.68E+02	6.41 %	5.76E+04	8.92E+03	15.48 %
	163.058	7.77E+03	7.19E+02	9.24 %	1.58E+05	1.56E+04	9.88 %
	169.059	3.55E+03	1.16E+02	3.27 %	5.75E+04	1.90E+03	3.30 %

Footnote.
[a] m/z^-_{obs}: observed mass to charge ratio.
[b] average peak area of three replicate samples.
[c] standard deviation (S.D.) and relative standard deviation (RSD%) of peak area. Relative standard deviation (RSD%) = S.D./Average × 100 %.
[d] average peak height of three replicate samples.
[e] standard deviation (S.D.) and relative standard deviation (RSD%) of peak height.
[f] $CH_3COCOOH$, molecular weight (MW) 88.06, 0.1 M solution, 1.5 h UV exposed [37].
[g] Mixture of 5 mM CHOCHO (MW 58.04) and 20 mM H_2O_2 (MW 34.01) solution, respectively, after 6 h UV exposure [43].
[h] 5 mM CHOCHO solution, MW58.04.
[i] synthetic oil-in-water emulsion, a 10 mL oil mixture consisted of 50 % diesel fuel marine, MIL-PRF-16884 N, 25 % 2190 TEP steam lube oil, MIL-PRF-17331K and 25 % 9250 diesel lube oil, MIL-PRF-9000L and 1 mL detergent mixture including type 1 general purpose detergent, MIL-D-16791G (1), 25 % commercial detergent Tide Ultra (liquid), and 25 % degreasing solvent, MIL-PRF-680C, Type III [44].
[j] $(CH_2)_4ON(CH_2)_3NH(CH_2)_2OCH_2CH_3$, MW 216.32 [36].

production of aqSOAs [40,43,66]. Indeed, several key compounds including glyoxal (m/z^- 57.03, $C_2HO_2^-$), $2H_2O...HCO_3$ anion (m/z^- 97.01, $CH_5O_5^-$), oligomers (m/z^- 158.06, $C_7H_{10}O_4^-$ and m/z^- 177.06, $C_{10}H_9O_3^-$) were identified. The replicate SIMS spectra in the mass range of m/z^- 50 − 200 are displayed in Fig. 3; and additional spectral mass range including all observed peaks are shown in Figs. S10–S11. The relative mass accuracy is within 20 ppm. Moreover, the RSDs% of peak areas and the corresponding peak height ratios observed in glyoxal and H_2O_2 samples are less than 5 %. The peak area and peak height of key compounds among pure reagent glyoxal solution, H_2O_2 solution, and the mixture of glyoxal and H_2O_2 were compared to identify the presence of product peaks as a result of photolysis reactions of the mixture.

The comparison results are summarized in Table 2, and the corresponding spectra were shown in Figs. 2–3). For example, the peak area/height of glyoxal (m/z^- 57.03) is highest in the glyoxal solution and lowest in the H_2O_2 solution. This indicates that glyoxal is consumed by H_2O_2 reactions. As to key products m/z^- 97.01, $CH_5O_5^-$, m/z^- 158.06, $C_7H_{10}O_4^-$, and m/z^- 177.06, $C_{10}H_9O_3^-$, the signal to noise ratios suggest that these peaks are below S/N compared against those in the glyoxal and H_2O_2 alone control samples. These findings indicate that these compounds are indeed formed due to photolysis of the glyoxal and H_2O_2 solution. These results show good data repeatability and reliable identification when static ToF-SIMS is applied. In brief, the replicate spectral analysis results of pyruvic acid (Fig. 2) and glyoxal (Fig. 3) indicate good data repeatability using static ToF-SIMS. It should be noted that VOC molecules evaporate in vacuum over time. However, the evaporation effect is small because key organic molecules could be observed in the PA and glyoxal samples. Additionally, the SIMS spectral repeatability of PA and glyoxal is satisfactory. Various samples give consistent satisfactory results using experimental systems, simulating atmospheric VOC transformations that led to aqSOA formation.

As to bilgewater emulsion samples, the main oil and detergent components are selected as the following: fatty acids (m/z^- 101.06, $C_5H_9O_2^-$), dicarbonic acid (m/z^- 104.98, $C_4H_9O_3^-$), benzoylformic acid (m/z^- 149.02, $C_8H_5O_3^-$), n-hexadecanoic acid (m/z^- 255.23, $C_{16}H_{31}O_2^-$), and tributyl phosphate (m/z^- 265.16, $C_{12}H_{26}O_4P^-$). These peaks are marked in Fig. 4 and the spectra in other mass ranges are shown in Figs. S12–S13. As shown in Table 1, the relative mass accuracy remains within in 20 ppm. On the other hand, the standard deviations of peak areas and heights were slightly larger than atmospheric samples (see Tables 2–3). This might be due to the complex components that exist in emulsion, which may cause a slight heterogeneity at the molecular scale. However, most RSDs% of the observed peak area and peak height ratios among the three replicates are less than 5 %. This finding indicates that static ToF-SIMS analysis can offer reproducible spectral results of rather complex oil-in-water emulsion mixtures.

Table 3
Comparisons of ratios of peak area and peak height of key products/fragments in the negative ion mode.

System	m/z^-_{obs}	Peak Area ratio[a]	Area ratio S. D.[b]	Area ratio RSD %[c]	Peak height ratio[d]	Peak height ratio S. D.[e]	Peak height ratio RSD %[f]
Pyruvic acid[g]	85.030	0.1560	0.0002	0.128 %	0.3523	0.0165	4.684 %
	113.023	0.2339	0.0012	0.513 %	0.2260	0.0112	4.956 %
	146.991	0.1523	0.0011	0.722 %	0.1324	0.0078	5.891 %
	175.040	0.2386	0.0035	1.467 %	0.2028	0.0050	2.465 %
	198.986	0.2191	0.0035	1.597 %	0.0866	0.0042	4.850 %
Glyoxal + H_2O_2[h]	57.028	0.7280	0.0089	1.223 %	0.8144	0.0020	0.246 %
	97.007	0.2209	0.0087	3.938 %	0.1644	0.0021	1.277 %
	158.057	0.0062	0.0003	4.839 %	0.0054	0.0002	3.704 %
	177.058*	0.0448	0.0005	1.116 %	0.0158	0.0002	1.266 %
Bilgewater emulsion[i]	101.058	0.1437	0.0118	8.212 %	0.0796	0.0034	4.271 %
	104.980	0.1030	0.0046	4.466 %	0.1268	0.0014	1.104 %
	149.022	0.3908	0.0147	3.762 %	0.4530	0.0020	0.442 %
	255.230*	0.2235	0.0106	4.743 %	0.1973	0.0135	6.842 %
	265.152	0.1391	0.0085	6.111 %	0.1433	0.0107	7.467 %
EMMPA[j]	73.042	0.1649	0.0108	6.549 %	0.1844	0.0176	9.544 %
	110.054*	0.1574	0.0136	8.640 %	0.1719	0.0215	12.51 %
	163.058	0.4651	0.0205	4.408 %	0.4722	0.0340	7.200 %
	169.059	0.2126	0.0022	1.035 %	0.1715	0.0052	3.032 %

Footnote:.
[a] average peak area ratio between the counts of specific peaks and total counts of all key products/fragments.
[b] standard deviation (S.D.) of peak area ratio.
[c] Relative standard deviation (RSD%) = S.D./Average × 100 %, RSD of the peak area ratio.
[d] average peak height ratio of three replicate samples.
[e] standard deviation (S.D.) of the peak height ratio.
[f] RSD of peak height ratio.
[g] $CH_3COCOOH$, molecular weight (MW) 88.06.
[h] 5 mM CHOCHO and 20 mM H_2O_2 solution, MW58.04 and 34.01, respectively.
[i] synthetic oil-in-water emulsion.
[j] $(CH_2)_4ON(CH_2)_3NH(CH_2)_2OCH_2CH_3$, MW 216.32.

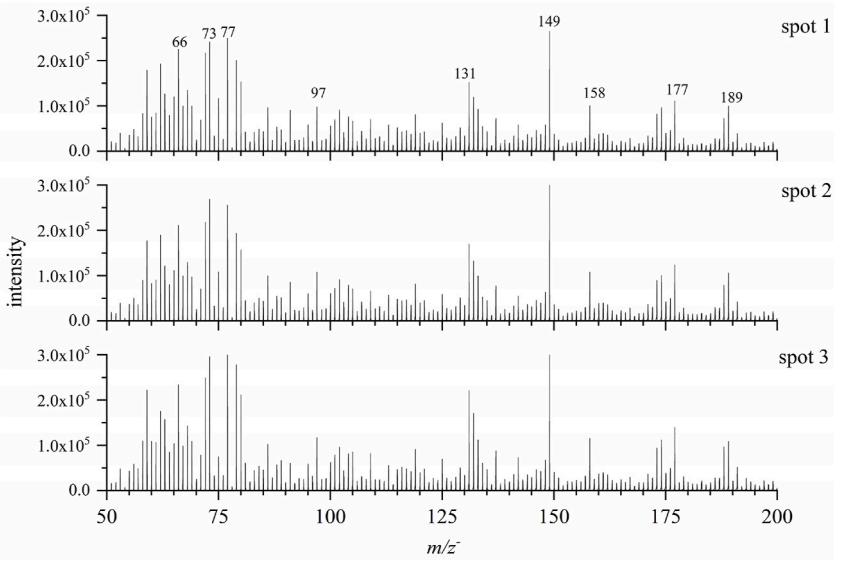

Fig. 3. SIMS spectral comparison of the glyoxal and H_2O_2 mixture solution showing representative peaks in the negative mode (m/z^- 50–200). Spots 1, 2, and 3 indicate consecutive measurements at three separate locations.

Fig. 5 exhibited SIMS spectral comparison of the CO_2 capture solvent 2-EMMPA in the negative mode. Additional spectral comparison results in other mass ranges are depicted in Figs. S14–S15. Four fragments of 2-EMMPA, namely $C_2H_3NO_2^-$ m/z^- 73.05, $CH_8N_3O_3^-$ m/z^- 110.06, $C_4H_9N_3O_4^-$ m/z^- 163.06, and $C_4H_{11}NO_6^-$ m/z^- 169.06, are used for spectral repeatability analysis. Like other environmental organic samples, the relative mass accuracy of key peaks is less than 20 ppm. Possible contaminants and fragments, such as m/z^- 133, show slight differences; however, the RSDs% of peak area and peak height ratios of most key compounds among the

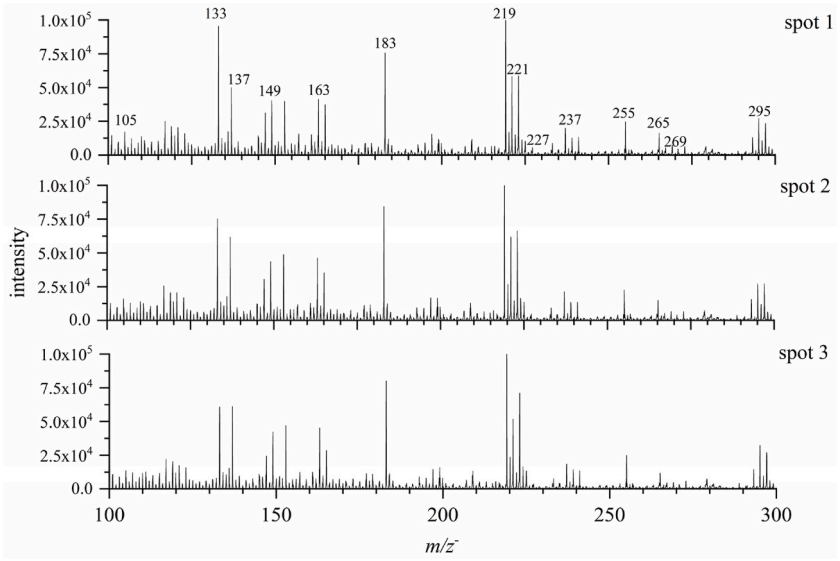

Fig. 4. SIMS spectral comparison of synthetic bilgewater emulsion showing representative peaks in the negative mode (m/z^- 100–300). Spots 1, 2, and 3 indicate consecutive measurements at three separate locations.

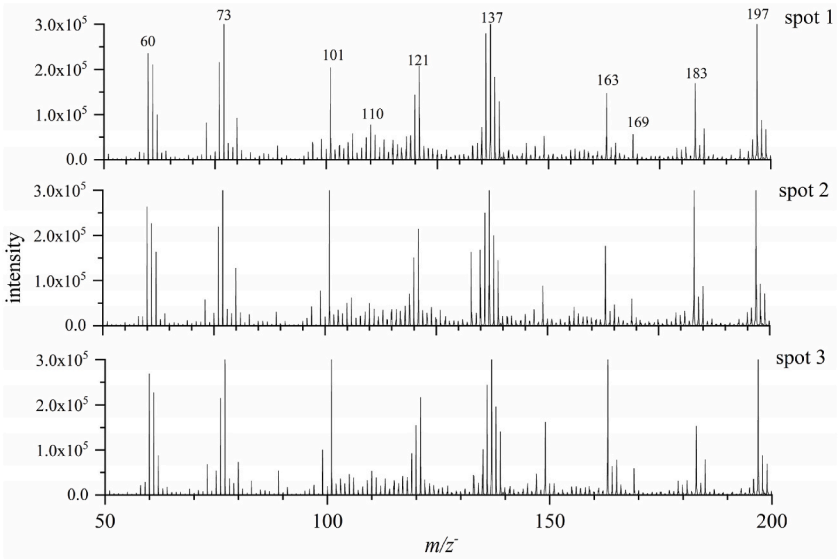

Fig. 5. SIMS spectral comparison of the CO_2 capture solvent EMMPA showing representative peaks in the negative mode (m/z^- 50–200). Spots 1, 2, and 3 indicate consecutive measurements at three separate locations.

three parallel samples are less than 10 % (as listed in Tables 2–3). Although the standard deviations of this capturing solvent are greater than other organic samples, the dataset's content is still considered to have good repeatability [67]. This is because the RSDs% are below 10 %. This higher standard deviation may be because the observed peaks are mainly fragments. Besides, the solvent synthesis process contains multi-steps, such as filtration and purification over a period of time; therefore, the interferences from synthesis and drying effect during sample preparation are unavoidable.

In summary, spectral repeatability is reasonable when static ToF-SIMS spectral measurements are applied to investigate environmental organics. The results are particularly impressive for the small VOC atmospheric models in the aqSOA transformation studies. As to other complicated organic compounds, the peak intensity seems to be influenced by the inevitable variance during synthesis, SIMS sample preparation, and the analysis process. Regardless, the main pseudomolecular peaks and fragment species can still be determined accurately.

3.2. SIMS spectral analysis in the positive ion mode

In the positive mode, four products, including biacetyl (m/z^+ 85.03, $C_4H_5O_2^+$), dehydration cluster ions (m/z^+ 113.03, $C_5H_5O_3^+$), 4, 5-Dioxo-4, 5-dihydro-3-furancarbaldehyde (m/z^+ 125.00, $C_5HO_4^+$) and 4-Methylumbelliferone (m/z^+ 176.05$C_{10}H_8O_3^+$), were used to compare spectral measurement repeatability in Fig. S4. SIMS spectral comparisons in other mass ranges are illustrated in Figs. S16–S17. Similarly to the negative mode, the relative mass accuracy is less than 20 ppm (Table S1) and the RSDs% of peak area ratios were smaller than 10 % (Tables S2–S3). For example, characteristic UV-induced oxidation products are glyoxal (m/z^+59.01, $C_2H_3O_2^+$), glycolic acid (m/z^+ 77.02, $C_2H_5O_3^+$), glycolaldehyde (m/z^+ 79.04, $C_2H_7O_3^+$), and oligomers (m/z^+ 153.13, $C_{10}H_{17}O^+$) in glyoxal UV aged samples. The spectra and statistical results are provided in Table S1 and Fig. S5, respectively. Additional spectra are shown in Figs. S18–S19. For compounds shown in the spectra, such as peaks m/z^+ 57, 69, 88 and 167, there is no appropriate identification related to glyoxal photochemical reactions within the uncertainty of relative mass accuracy (i.e., 20 ppm). Thus, these peaks were considered as molecular fragments, i.e., $C_2HO_2^+$, $C_4H_5O^+$, $C_2O_4^+$ and $C_{13}H_{11}^+$, respectively. The peak intensities show a greater percentage difference in the positive mode than the negative mode. However, as a surface sensitive, semi-quantitative analytical tool, these products could still be identified effectively in SIMS spectral analysis as shown in Table S1 and Figs. S18–S19. In fact, SIMS offers superior surface sensitivity compared to bulk techniques like gas chromatograph – mass spectrometry (GC-MS) or liquid chromatograph – mass spectrometry (LC-MS) in terms of speciation of oxidation products in SOA formation [68,69]. The characteristic peaks in bilgewater emulsions are phenethyl (m/z^+ 107.09, $C_8H_{11}^+$), phenylpropyl (m/z^+ 119.09, $C_9H_{11}^+$), hydroxytyrosol (m/z^+ 153.06, $C_8H_9O_3^+$), aminoacetate (m/z^+ 191.03, $C_5H_7N_2O_6^+$), and fragments (m/z^+ 243.10, $C_7H_{17}N_2O_8^+$). The replicate spectral comparison is illustrated in Fig. S6. Other supporting mass spectra are depicted in Figs. S20–S21. As shown in Table S1, the relative mass accuracy remains within 20 ppm; and the RSDs% of peak areas and their ratios are smaller than 10 %. Slightly larger RSDs% of the emulsions are likely due to the complex components that exist in the organic mixtures than those of simpler VOC systems in the positive mode. It is notable that peaks occurring with a $\Delta m/z$ 44 amu difference starting from m/z^+ 463 to m/z^+ 771 (shown in Fig. S21). This implies that CO_2 could be absorbed on the bilgewater emulsion in the form of $C_{26+n}H_{32}O_{6+2n}Na^+$ (relative mass accuracy <20 ppm, n = 0–7).

For the CO_2 capture solvent EMMPA, seven typical fragments are chosen for spectral repeatability analysis, including $C_6H_{14}N_3^+$ m/z^+ 128.12, $C_8H_{16}N_3^+$ m/z^+ 154.13, $C_8H_{18}N_3O^+$ m/z^+ 172.14, $C_9H_{18}N_3O^+$ m/z^+ 184.15, $C_{11}H_{25}N_2O_2^+$ m/z^+ 216.19, $C_{12}H_{25}N_2O_2^+$ m/z^+ 229.19, and $C_{11}H_{25}N_2O_4^+$ m/z^+ 216.18. The spectral comparison results are depicted in Fig. S7; and other mass ranges are illustrated in Figs. S22–S23. Like other environmental organic systems, the relative mass accuracy of characteristic peaks is smaller than 20 ppm. It should be noted that the RSDs% based on peak area ratios of all EMMPA fragments are less than 10 % as shown in Tables S2–S3, smaller than those in the negative mode. This comparison indicates that the ion yields of positive EMMPA fragment ions are more repeatable than negative ones. Whereas the peak areas' standard deviations of glyoxal, pyruvic acid, and bilgewater emulsions in the positive mode are all slightly greater than those in the negative mode. The different RSDs% in the positive and negative mode might be because these ions have different trajectories (shown in Fig. 1b), which cause intensity differences between the positive and negative mode. This finding suggests that both ion modes should be used when analyzing complex organics to obtain complementary data and more signature signals of such systems.

3.3. SIMS mass spectral repeatability

The spectral repeatability results show that the application of static ToF-SIMS is suitable to study environmental organics. It offers high mass relative accuracy in both negative and positive ion modes. For ToF-SIMS spectral analysis, the mass resolution and accuracy are directly related to the primary ion beam width as well as sputtering and extraction processes. The good repeatability reveals that the narrower Bi_3^+ beam width, for instance a pulse width of around 0.8 ns, is a desirable choice for environmental organics analysis. Moreover, our previous studies suggest that the beam damage induced by Bi_3^+ has less influence on organic samples, whereas Bi^+ beam damage cannot be neglected [24]. Besides, the Bi_3^+ beam is more sensitive for macromolecules than Bi^+. Such feature can enhance peak intensity by several orders of magnitudes. Thus, it reduces the interference caused by system noise, especially in the positive mode [10,11,13,24,70].

The ion yields of secondary ions can significantly be influenced by sample atomic mixing, surface roughness, and uniformity [71–73]. The discrepancy and consistency of sample surfaces may cause peak area or height differences, thereby affecting relative mass accuracy and peak area/height measurement ratios. During analysis and detection, the spectral signals depend not only on their intrinsic attributes but also sample preparation process. Our results show that ToF-SIMS can provide strong and stable signals for both simple and complex mixture components of environmental significance in the negative ion mode. As to the positive mode, peak intensities show a higher relative difference except for the EMMPA solvent. However, characteristic ion signals can still be detected and identified readily. The peak area and peak height ratios shown in Tables 3 and S3 suggest that fragments of low volatility oligomers formed from photochemical reactions of small atmospheric VOCs (i.e., glyoxal, pyruvic acid) are more likely to be detected using the Bi_3^+ primary ion beam. For bilgewater emulsions and EEPMA samples, more fragments and products from smaller molecules could be observed with higher intensity (i.e., $C_4H_9N_3O_4^-$ m/z^- 163.06, $C_8H_{18}N_3O^+$ m/z^+ 172.14 in EMMPA). This finding indicates that secondary ions generated by the primary ion beam mainly consist of smaller molecular components or their fragments from organic mixtures.

The fact that key compounds could be identified with a less than 20 ppm relative mass accuracy indicates that environmental organic materials could be analyzed using static ToF-SIMS effectively. The RSDs% of peak area/height were slightly larger when complex components exist in organic samples. However, these products could still be identified clearly in the SIMS spectra, for instance

in the bilgewater case. Furthermore, identification of outliers is helpful for speciation and subsequent analysis. Compared raw intensities, peak ratios of key fragments or products have smaller RSDs%, providing valuable information for identification of organic compounds. Based on observations of multiple systems, it is recommended that the pulsed 25 keV Bi_3^+ is suitable for environmental organic analysis. Specifically, the high mass relative accuracy of SIMS spectral analysis allows us to distinguish complex composition of environmental samples with reasonable confidence. Another advancement using SIMS is that the good repeatability of signal intensity can reduce peak identification error by comparing replicate plots.

In summary, ToF-SIMS detection, with the instrument development in recent decades, can provide more insights into components, dynamics, and reaction mechanisms on environmental organics by taking advantage of high mass resolution, high sensitivity, mass range, and good repeatability offered by static SIMS analysis. Besides instrument efficiency (e.g., micro channel plate condition), deviation of ion fragments generated from different kinds of molecules can be influenced by minor surface topography easily, which causes slightly higher RSD% than quasi-molecular ions. Appropriate sample preparation, normalization, and identification of outliers are helpful strategies to reduce the deviation from surface topography and instrument efficiency.

4. Conclusions

Sample preparation is crucial to acquire reliable and reproducible results in ToF-SIMS. Moreover, the sample preparation processes summarized in this study has turned out to offer an appropriate baseline approach for static ToF-SIMS analysis. Our results provide a reliable set of conditions to investigate environmental organic samples using static ToF-SIMS. To the best of our knowledge, this work has presented the first set of SIMS static analysis of environmental organics. Because these systems of interest are so diverse and they follow different reaction mechanisms, the distribution of percentage of products vs. reactants would not be the same. The Bi_3^+ primary ion beam is known to be suitable for research of organic samples such as polymers, thin films, organic electronics, and industrial samples [33,35]. Our results show that it is also a good choice for studying environmental organics. Additional in situ liquid SIMS research of these environmental systems have been performed or ongoing. More studies would be needed on organic samples using static and liquid ToF-SIMS to further evaluatation of spectral repeatability because there is a lack of existing literature of environmentally relevant organics. With the advancement of SIMS, such as mass spectrometry (MS)-MS, giant cluster ion beam (GCIB)-SIMS, and liquid SIMS, it is anticipated that ToF-SIMS can play a more significant role and provide more useful information in the studies of environmental organics in the real world in the future.

Ethical statement

The authors declare that no human or animal studies appeared in this paper. Also, no clinical trials were described in this work.

Data availability statement

The data that support the findings of this study are available from the corresponding author upon reasonable request. Data is also available from Dr. Yu's github, git@code.ornl.gov:nsrd_au/data_pub_sharing.git.

Funding

Funding for Xiao Sui was provided by Natural Science Foundation of Shandong Province, grant number ZR2022QB137. Experimental efforts were supported by the strategic Laboratory Directed Research and Development (LDRD) of the Physical Sciences Directorate of the Oak Ridge National Laboratory (ORNL). Preparation of the manuscript was supported partially by the U. S. Department of Energy (DOE) Environmental Management (EM) program award 277636.

CRediT authorship contribution statement

Xiao Sui: Writing – review & editing, Writing – original draft, Investigation, Formal analysis, Data curation, Methodology, Validation, Visualization. **Xiao-Ying Yu:** Writing – review & editing, Writing – original draft, Validation, Supervision, Software, Resources, Project administration, Methodology, Investigation, Funding acquisition, Formal analysis, Data curation, Conceptualization.

Declaration of competing interest

The authors declare that they have no known competing financial interests or personal relationships that could have appeared to influence the work reported in this paper.

Acknowledgements

Oak Ridge National Laboratory (ORNL) is managed by UT-Battelle, LLC, for the U. S. Department of Energy (DOE) under contract number DE-AC05-00OR22725. The United States Government retains and the publisher, by accepting the article for publication, acknowledges that the United States Government retains a non-exclusive, paid-up, irrevocable, world-wide license to publish or reproduce the published form of this manuscript, or allow others to do so, for United States Government purposes. The Department of

Energy will provide public access to these results of federally sponsored research in accordance with the DOE Public Access Plan (http://energy.gov/downloads/doe-public-access-plan).

Appendix A. Supplementary data

Supplementary data to this article can be found online at https://doi.org/10.1016/j.heliyon.2024.e37913.

References

[1] A. Nel, Air pollution–related illness: effects of particles, Science 308 (2005) 804–805.
[2] E.G. Stephanou, The decay of organic aerosols, Nature 434 (2005), 31-31.
[3] J. Gao, Y. Zhang, J. Son, J.E. Bara, K.E. O'Harra, M.H. Engelhard, D.J. Heldebrant, R. Rousseau, X.-Y. Yu, separation membrane and capture solvents The interfacial compatibility between a potential CO_2, Carbon Capture Science & Technology 2 (2022) 100037.
[4] X.-Y. Yu, J. Yao, D.B. Lao, D.J. Heldebrant, Z. Zhu, D. Malhotra, M.-T. Nguyen, V.-A. Glezakou, R. Rousseau, Mesoscopic structure facilitates rapid CO_2 transport and reactivity in CO_2 capture solvents, J. Phys. Chem. Lett. 9 (2018) 5765–5771.
[5] J. Yao, D.B. Lao, X. Sui, Y. Zhou, S.K. Nune, X. Ma, T.P. Troy, M. Ahmed, Z. Zhu, D.J. Heldebrant, et al., Two coexisting liquid phases in switchable ionic liquids, Phys. Chem. Chem. Phys. 19 (2017) 22627–22632.
[6] X.H. Liu, C.Z. Guan, S.Y. Ding, W. Wang, H.J. Yan, D. Wang, L.J. Wan, On-surface synthesis of single-layered two-dimensional covalent organic frameworks via solid-vapor interface reactions, J. Am. Chem. Soc. 135 (2013) 10470–10474.
[7] X. Yan, R.M. Bain, R.G. Cooks, Organic reactions in microdroplets: reaction acceleration revealed by mass spectrometry, Angewandte Chemie International edition 55 (2016) 12960–12972.
[8] C. Qu, M. Ma, W. Chen, P. Cai, X.-Y. Yu, X. Feng, Q. Huang, Modeling of Cd adsorption to goethite-bacteria composites, Chemosphere 193 (2018) 943–950.
[9] L. Van Vaeck, A. Adriaens, R. Gijbels, Static secondary ion mass spectrometry (S-SIMS) Part 1: methodology and structural interpretation, Mass Spectrom. Rev. 18 (1999) 1–47.
[10] L. Yang, X.Y. Yu, Z. Zhu, M.J. Iedema, J.P. Cowin, Probing liquid surfaces under vacuum using SEM and ToF-SIMS, Lab Chip 11 (2011) 2481–2484.
[11] L. Yang, X.Y. Yu, Z. Zhu, T. Thevuthasan, J.P. Cowin, Making a hybrid microfluidic platform compatible forin situimaging by vacuum-based techniques, J. Vac. Sci. Technol. A 29 (2011) 061101.
[12] S. Sabale, D. Barpaga, J. Yao, L. Kovarik, Z. Zhu, S. Chatterjee, B.P. McGrail, R.K. Motkuri, X.Y. Yu, Understanding time dependence on zinc metal-organic framework growth using in situ liquid secondary ion mass spectrometry, ACS Applied Material Interfaces 12 (2020) 5090–5098.
[13] B. Liu, X.Y. Yu, Z. Zhu, X. Hua, L. Yang, Z. Wang, In situ chemical probing of the electrode-electrolyte interface by ToF-SIMS, Lab Chip 14 (2014) 855–859.
[14] L. Yang, Z. Zhu, X.-Y. Yu, S. Thevuthasan, J.P. Cowin, Performance of a microfluidic device for in situ ToF-SIMS analysis of selected organic molecules at aqueous surfaces, Anal. Methods 5 (2013) 2515.
[15] L. Yang, Z. Zhu, X.-Y. Yu, E. Rodek, L. Saraf, T. Thevuthasan, J.P. Cowin, In situ SEM and ToF-SIMS analysis of IgG conjugated gold nanoparticles at aqueous surfaces, Surf. Interface Anal. 46 (2014) 224–228.
[16] X. Hua, M.J. Marshall, Y. Xiong, X. Ma, Y. Zhou, A.E. Tucker, Z. Zhu, S. Liu, X.Y. Yu, Two-dimensional and three-dimensional dynamic imaging of live biofilms in a microchannel by time-of-flight secondary ion mass spectrometry, Biomicrofluidics 9 (2015) 031101.
[17] H. Rensmo, H. Siegbahn, Photoelectron spectroscopy for chemical analysis, Chimia 69 (2015) 22.
[18] A. Benninghoven, Surface investigation of solids by the statical method of secondary ion mass spectroscopy (SIMS), Surf. Sci. 35 (1973) 427–457.
[19] I.S. Gilmore, M.P. Seah, Static SIMS inter-laboratory study, Surf. Interface Anal. 29 (2000) 624–637.
[20] A.M. Belu, D.J. Graham, D.G. Castner, Time-of-flight secondary ion mass spectrometry: techniques and applications for the characterization of biomaterial surfaces, Biomaterials 24 (2003) 3635–3653.
[21] R.V. Ham, L.V. Vaeck, A. Adriaens, F. Adams, Static secondary ion mass spectrometry for organic and inorganic molecular analysis in solids, Anal. Chim. Acta 500 (2003) 259–278.
[22] J.S. Fletcher, S. Rabbani, A.M. Barber, N.P. Lockyer, J.C. Vickerman, Comparison of C_{60} and GCIB primary ion beams for the analysis of cancer cells and tumour sections, Surf. Interface Anal. 45 (2012) 273–276.
[23] J.S. Fletcher, Latest applications of 3D ToF-SIMS bio-imaging, Biointerphases 10 (2015), 018902-018901-018902-018908.
[24] Y. Zhou, J. Yao, Y. Ding, J. Yu, X. Hua, J.E. Evans, X. Yu, D.B. Lao, D.J. Heldebrant, S.K. Nune, et al., Improving the molecular ion signal intensity for in situ liquid SIMS analysis, J. Am. Soc. Mass Spectrom. 27 (2016) 2006–2013.
[25] I.S. Gilmore, M.P. Seah, F.M. Green, Static TOF-SIMS — a VAMAS interlaboratory study. Part I. Repeatability and reproducibility of spectra, Surf. Interface Anal. 37 (2005) 651–672.
[26] N. Winograd, Z. Postawa, J. Cheng, C. Szakal, J. Kozole, B.J. Garrison, Improvements in SIMS continue is the end in sight? Appl. Surf. Sci. 252 (2006) 6836–6843.
[27] P. Kingshott, G. Andersson, S.L. McArthur, H.J. Griesser, Surface modification and chemical surface analysis of biomaterials, Curr. Opin. Chem. Biol. 15 (2011) 667–676.
[28] J.S. Fletcher, J.C. Vickerman, A new SIMS paradigm for 2D and 3D molecular imaging of bio-systems, Anal. Bioanal. Chem. 396 (2010) 85–104.
[29] V.S. Smentkowski, G. Zorn, A. Misner, G. Parthasarathy, A. Couture, E. Tallarek, B. Hagenhoff, ToF-SIMS depth profiling of organic solar cell layers using an Ar cluster ion source, J. Vac. Sci. Technol. A 31 (2013) 030601.
[30] W. Wei, Y. Zhang, R. Komorek, A. Plymale, R. Yu, B. Wang, Z. Zhu, F. Liu, X.Y. Yu, Characterization of syntrophic Geobacter communities using ToF-SIMS, Biointerphases 12 (2017) 05G601.
[31] Y. Ding, Y. Zhou, J. Yao, Y. Xiong, Z. Zhu, X.Y. Yu, Molecular evidence of a toxic effect on a biofilm and its matrix, Analyst 144 (2019) 2498–2503.
[32] Y. Zhang, R. Komorek, J. Son, S. Riechers, Z. Zhu, J. Jansson, C. Jansson, X.Y. Yu, Molecular imaging of plant-microbe interactions on the Brachypodium seed surface, Analyst 146 (2021) 5855–5865.
[33] X. Hua, X.Y. Yu, Z. Wang, L. Yang, B. Liu, Z. Zhu, A.E. Tucker, W.B. Chrisler, E.A. Hill, T. Thevuthasan, et al., In situ molecular imaging of a hydrated biofilm in a microfluidic reactor by ToF-SIMS, Analyst 139 (2014) 1609–1613.
[34] W. Wei, A. Plymale, Z. Zhu, X. Ma, F. Liu, X.Y. Yu, In vivo molecular insights into syntrophic geobacter aggregates, Anal. Chem. 92 (2020) 10402–10411.
[35] Y. Ding, Y. Zhou, J. Yao, C. Szymanski, J. Fredrickson, L. Shi, B. Cao, Z. Zhu, X.Y. Yu, In situ molecular imaging of the biofilm and its matrix, Anal. Chem. 88 (2016) 11244–11252.
[36] J. Son, Y. Shen, J. Yao, D. Paynter, X.-Y. Yu, Surface evolution of synthetic bilgewater emulsion, Chemosphere 236 (2019) 124345.
[37] Y. Fu, Y. Zhang, F. Zhang, J. Chen, Z. Zhu, X.-Y. Yu, Does interfacial photochemistry play a role in the photolysis of pyruvic acid in water? Atmos. Environ. 191 (2018) 36–45.
[38] X. Sui, Y. Zhou, F. Zhang, Y. Zhang, J. Chen, Z. Zhu, X.Y. Yu, ToF-SIMS characterization of glyoxal surface oxidation products by hydrogen peroxide: a comparison between dry and liquid samples, Surf. Interface Anal. 50 (2017) 927–938.
[39] W. Li, H. Li, J. Li, X. Cheng, Z. Zhang, F. Chai, H. Zhang, T. Yang, P. Duan, D. Lu, et al., TOF-SIMS surface analysis of chemical components of size-fractioned urban aerosols in a typical heavy air pollution event in Beijing, Journal of Environmental Science 69 (2018) 61–76.

[40] X. Sui, Y. Zhou, F. Zhang, J. Chen, Z. Zhu, X.Y. Yu, Deciphering the aqueous chemistry of glyoxal oxidation with hydrogen peroxide using molecular imaging, Phys. Chem. Chem. Phys. 19 (2017) 20357–20366.
[41] F. Zhang, X. Yu, X. Sui, J. Chen, Z. Zhu, X.-Y. Yu, Evolution of aqSOA from the air-liquid interfacial photochemistry of glyoxal and hydroxyl radicals, Environ. Sci. Technol. 53 (2019) 10236–10245.
[42] J. Kothandaraman, J.S. Lopez, Y. Jiang, E.D. Walter, S.D. Burton, R.A. Dagle, D.J. Heldebrant, Integrated capture and conversion of CO_2 to methanol in a post-combustion capture solvent: heterogeneous catalysts for selective C-N bond cleavage, Adv. Energy Mater. 12 (2022) 2202369.
[43] X. Sui, B. Xu, J. Yao, O. Kostko, M. Ahmed, X.Y. Yu, New insights into secondary organic aerosol formation at the air-liquid interface, J. Phys. Chem. Lett. 12 (2021) 324–329.
[44] Y. Shen, J. Yao, J. Son, Z. Zhu, X.Y. Yu, Liquid ToF-SIMS revealing the oil, water, and surfactant interface evolution, Phys. Chem. Chem. Phys. 22 (2020) 11771–11782.
[45] Y. Shen, Y. Fu, J. Yao, D. Lao, S. Nune, Z. Zhu, D. Heldebrant, X. Yao, X.Y. Yu, Revealing the structural evolution of green rust synthesized in ionic liquids by in situ molecular imaging, Adv. Mater. Interfac. 7 (2020) 2000452.
[46] I.S. Gilmore, F.M. Green, M.P. Seah, Static Tof-Sims, A VAMAS interlaboratory study. Part II - accuracy of the mass scale and G-SIMS compatibility, Surf. Interface Anal. 39 (2007) 817–825.
[47] F.M. Green, I.S. Gilmore, M.P. Seah, Mass accuracy—tof-SIMS, Appl. Surf. Sci. 252 (2006) 6591–6593.
[48] W. Kern, The evolution of silicon wafer cleaning Technology, J. Electrochem. Soc. 137 (1990) 1887–1892.
[49] A.G. Carlton, B.J. Turpin, K.E. Altieri, S. Seitzinger, A. Reff, H.-J. Lim, B. Ervens, Atmospheric oxalic acid and SOA production from glyoxal: results of aqueous photooxidation experiments, Atmos. Environ. 41 (2007) 7588–7602.
[50] Y.B. Lim, Y. Tan, M.J. Perri, S.P. Seitzinger, B.J. Turpin, Aqueous chemistry and its role in secondary organic aerosol (SOA) formation, Atmos. Chem. Phys. 10 (2010) 10521–10539.
[51] J. Reader, C.J. Sansonetti, J.M. Bridges, Irradiances of spectral lines in mercury pencil lamps, Appl. Opt. 35 (1996) 78–83.
[52] J. Church, D.M. Paynter, W.H. Lee, In situ characterization of oil-in-water emulsions stabilized by surfactant and salt using microsensors, Langmuir 33 (2017) 9731–9739.
[53] D. Malhotra, D.C. Cantu, P.K. Koech, D.J. Heldebrant, A. Karkamkar, F. Zheng, M.D. Bearden, R. Rousseau, V.-A. Glezakou, Directed hydrogen bond placement: low viscosity amine solvents for CO_2 capture, ACS Sustain. Chem. Eng. 7 (2019) 7535–7542.
[54] F. Zheng, D.J. Heldebrant, P.M. Mathias, P. Koech, M. Bhakta, C.J. Freeman, M.D. Bearden, A. Zwoster, Bench-scale testing and process performance projections of CO_2 capture by CO_2–binding organic liquids (CO_2BOLs) with and without polarity-swing-assisted regeneration, Energy Fuels 30 (2016) 1192–1203.
[55] E.D. Walter, D. Zhang, Y. Chen, K. Sung Han, J.D. Bazak, S. Burton, K. O'Harra, D.W. Hoyt, J.E. Bara, D. Malhotra, et al., Enhancing CO_2 transport across a PEEK-ionene membrane and water-lean solvent interface, ChemSusChem (2023) e202300157.
[56] A. Priebe, T. Xie, G. Bürki, L. Pethö, J. Michler, The matrix effect in TOF-SIMS analysis of two-element inorganic thin films, J. Anal. Atomic Spectrom. 35 (2020) 1156–1166.
[57] F. Kollmer, N. Bourdos, R. Kamischke, A. Benninghoven, Nonresonant Laser-SNMS and TOF-SIMS analysis of sub-μm structure, Appl. Surf. Sci. 203–204 (2003) 238–243.
[58] J. Yu, Y. Zhou, M. Engelhard, Y. Zhang, J. Son, S. Liu, Z. Zhu, X.Y. Yu, In situ molecular imaging of adsorbed protein films in water indicating hydrophobicity and hydrophilicity, Sci. Rep. 10 (2020) 3695.
[59] C.E. Zwilling, M.Y. Wang, Covariance based outlier detection with feature selection, Annu Int Conf IEEE Eng Med Biol Soc 2016 (2016) 2606–2609.
[60] H. Zhou, H. Ren, P. Royer, H. Hou, X.-Y. Yu, Big data analytics for long-term meteorological observations at hanford site, Atmosphere 13 (2022) 136.
[61] J. Osborne, in: J. Osborne (Ed.), Best Practices in Quantitative Methods, Sage Research Methods, Thousand Oaks, California, 2008.
[62] P. Blainey, M. Krzywinski, N. Altman, Replication, Nat. Methods 11 (2014) 879–880.
[63] R.C. Deng, P. Williams, Factors affecting precision and accuracy in quantitative analysis by secondary ion mass spectrometry, Anal. Chem. 61 (1989) 1946–1948.
[64] D.L. Tabb, L. Vega-Montoto, P.A. Rudnick, A.M. Variyath, A.-J.L. Ham, D.M. Bunk, L.E. Kilpatrick, D.D. Billheimer, R.K. Blackman, H.L. Cardasis, et al., Repeatability and reproducibility in proteomic identifications by liquid chromatography-tandem mass spectrometry, J. Proteome Res. 9 (2010) 761–776.
[65] C. Yang, W. Wei, F. Liu, X.Y. Yu, Peak selection matters in principal component analysis: a case study of syntrophic microbes, Biointerphases 14 (2019) 051004.
[66] F. Zhang, X. Yu, J. Chen, Z. Zhu, X.-Y. Yu, Dark air–liquid interfacial chemistry of glyoxal and hydrogen peroxide, npj Climate and Atmospheric Science 2 (2019).
[67] H. Min, J.-W. Park, H.K. Shon, D.W. Moon, T.G. Lee, ToF-SIMS study on the cleaning methods of Au surface and their effects on the reproducibility of self-assembled monolayers, Appl. Surf. Sci. 255 (2008) 1025–1028.
[68] J.B. Gilman, B.M. Lerner, W.C. Kuster, P.D. Goldan, C. Warneke, P.R. Veres, J.M. Roberts, J.A. de Gouw, I.R. Burling, R.J. Yokelson, Biomass burning emissions and potential air quality impacts of volatile organic compounds and other trace gases from fuels common in the US, Atmos. Chem. Phys. 15 (2015) 13915–13938.
[69] Q.F. He, X. Ding, X.M. Wang, J.Z. Yu, X.X. Fu, T.Y. Liu, Z. Zhang, J. Xue, D.H. Chen, L.J. Zhong, et al., Organosulfates from pinene and isoprene over the Pearl River Delta, South China: seasonal variation and implication in formation mechanisms, Environ. Sci. Technol. 48 (2014) 9236–9245.
[70] R. Shishido, M. Mitsuishi, S. Suzuki, Effects of polymer crystallization on the molecular sensitivity in TOF-SIMS measurements using Bi_1+ and Bi_3^{2+} ions, J. Vac. Sci. Technol. B 38 (2020) 034004.
[71] B. Fares, B. Gautier, J.C. Dupuy, G. Prudon, P. Holliger, Deconvolution of very low primary energy SIMS depth profiles, Appl. Surf. Sci. 252 (2006) 6478–6481.
[72] G.S. Lau, E.S. Tok, R. Liu, A.T.S. Wee, J. Zhang, Roughening behavior in Si/SiGe heterostructures under O_2+ bombardment, Nucl. Instrum. Methods Phys. Res. Sect. B Beam Interact. Mater. Atoms 215 (2004) 76–82.
[73] X.L. Yan, M.M. Duvenhage, J.Y. Wang, H.C. Swart, J.J. Terblans, Evaluation of sputtering induced surface roughness development of Ni/Cu multilayers thin films by Time-of-Flight Secondary Ion Mass Spectrometry depth profiling with different energies O_2^+ ion bombardment, Thin Solid Films 669 (2019) 188–197.